LAWRENCE
LIVERMORE
NATIONAL
LABORATORY

LLNL-PROC-410508

Temperature measurement through detailed balance in X-ray Thomson scattering

T. Doppner, O. L. Landen, H. J. Lee, P. Neumayer, S. P. Regan, S. H. Glenzer

February 11, 2009

Radiative Properties of Hot Dense Matter 2008
Santa Barbara, CA, United States
November 10, 2008 through November 14, 2008

Disclaimer

Temperature measurement through detailed balance in X-ray Thomson scattering

T. Döppner[a], O.L. Landen[a], H.J. Lee[b], P. Neumayer[a], S.P. Regan[c], S.H. Glenzer[a]

[a] *Lawrence Livermore National Laboratory, P.O. Box 808, Livermore, CA 94551, USA*
[b] *University of California, Berkeley, CA 94720, USA*
[c] *Laboratory for Laser Energetics, University of Rochester, 250 East River Road, Rochester, New York 14623-1299, USA*

Abstract

The plasma conditions in isochorically heated beryllium are measured by x-ray Thomson scattering in the collective regime with a Cl Ly-α x-ray source at 2.96 keV. In addition to the down–shifted plasmon shape which provides electron density and temperature information, an up–shifted plasmon signal is observed allowing a model independent determination of the plasma temperature from the detailed balance relation.

Key words: Warm dense matter, Plasma diagnostic, Thomson scattering, Plasmons
PACS: 52.25.Os 52.35.Fp 71.45.Gm 71.10.Ca

1. Introduction

Accurate characterization of warm dense matter is important for inertial confinement fusion and high energy density physics experiments [1, 2]. In particular, the capability to measure electron temperature and density in dense matter allows us to test dense plasma modeling. X–ray Thomson scattering has been developed on the Omega laser facility employing isochorically heated [3, 4] and laser shock-compressed matter [5], and more recently also on medium sized laser facilities [2]. For a recent review see Ref. [6]. These experiments access matter at solid density and above approaching electron densities of $n_e = 10^{24}/cm^3$. Besides demonstrating the diagnostic capability for future studies, e.g., on the National Ignition Facility, present experiments address fundamental physics questions such as the equation of state in dense matter, structure factors in two-component plasmas, limits of the validity of the random phase approximation, and the role of collisions. X-ray scattering experiments employ powerful laser-produced x-ray sources that penetrate through dense and compressed materials with densities of solid and above. Ly-α or He-α radiation from nanosecond laser plasmas have been applied at moderate x-ray energies of E = 3 - 9 keV that fulfill the stringent requirements on photon numbers and bandwidth for spectrally-resolved x-ray scattering measurements in single shot experiments. Experiments have been performed in the noncollective and collective scattering regime. In backscattering geometry the plasma is probed in the non–collective scattering regime yielding the down–shifted Compton line that is broadened by the thermal motion of the electrons [3]. In contrast, in a forward scattering geometry plasmons, i.e. electron density oscillations, are observed [4]. From the detailed balance , i.e. the ratio of the up–shifted to the down–shifted plasmon, the plasma temperature can be determined from first principles [6, 7]. The detailed balance relation can be written as [7, 8]

$$\frac{S(-\mathbf{k},-\omega)}{S(\mathbf{k},\omega)} = \exp\left(-\frac{\hbar\omega}{kT}\right) \quad (1)$$

with $S(\mathbf{k},\omega)$ the dynamic structure factor, which is proportional to the inelastically scattered x–ray signal, $\hbar\omega$ the energy transfer of the scattered photons and T the equilibrium temperature of the system. For this relation to hold true no other assumption than thermal equilibrium has to be made. This makes temperature measurements based on this detailed balance a very powerful tool since it does not rely on any model assumptions.

2. Experimental setup

A new collective scattering experiment was performed at the Omega laser facility at the Laboratory for Laser Energetics at the University of Rochester. A schematic of the target and the laser beam configuration is shown in Fig. 1. To isochorically heat a 250 μm Be foil with 3.4-3.6 keV Ag L-shell radiation (see Fig. 2), 10 drive beams with a total energy of 4.7 kJ

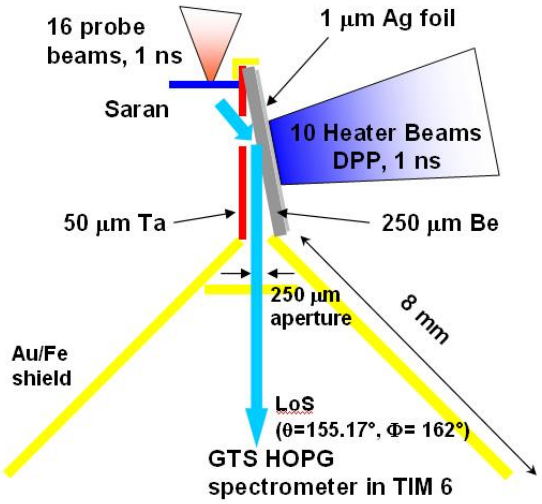

Figure 1: Schematic of the experimental setup. 10 heater beams generate Ag L-shell x rays which isochorically heat a 250 μm Be foil. 16 delayed probe beams create a Cl Ly-α x-ray backlighter at 2.96 keV to probe the plasma conditions. For beam timing see Fig. 2.

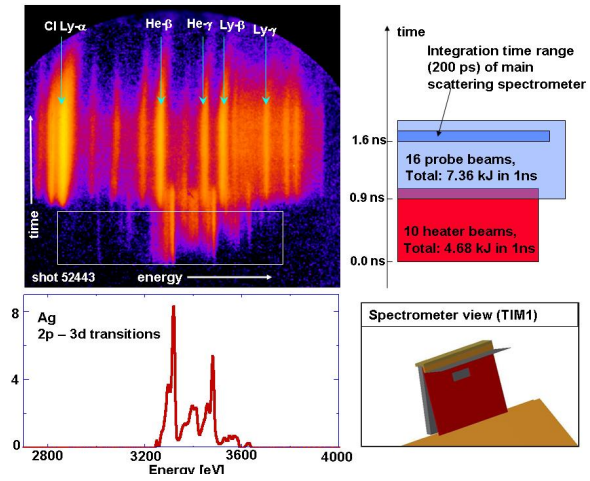

Figure 2: Streaked x-ray spectrum which illustrates the beam timing for shot 52443 as given in the right column. Early Ag L-shell radiation is generated by the heater beams, while the probe beams causes emission of several helium and hydrogen like lines of Cl. Note that the Ag L–shell emission is observed in transmission through the 250 μm Be foil.

at 351 nm in a 1 ns pulse width were incident on a 1 μm silver foil glued to the Be. Distributed phase plates (DPP, type SG4) were used to achieve a smooth beam spot with a diameter of 800 μm yielding a drive intensity of 7×10^{14} W/cm^2. To generate the x-ray probe 16 beams with a total energy of 7.36 kJ at 351 nm were focused to a 150 μm spot on a 12 μm Saran foil to create Cl Ly-α at 2.96 keV. The source spectrum was determined in a dedicated disk shot, see Fig. 4. Besides the Cl Ly-α line a satellite, down–shifted by 30 eV, is emitted. The contrast between the main source line and the red–shifted satellite is 10. The x–ray photons are collimated by a 50 μm thick Ta pinhole to define the scattering to 40°, which limits the solid angle of the source to XY sterrad. Both the backlighter performance and the Ag L–shell emission are monitored by a streaked crystal spectrometer, see Fig. 2. The main contribution to the Ag foil emission stems from 3d–2p transitions in the energy range between 3.4 and 3.6 keV. In the energy range of the x-ray source line used for the Thomson scattering measurement no significant contribution from Ag emission is observed. In addition, the L-shell emission turns off promptly after the end of the heater beams. This allows us to probe the plasma conditions very close to the end of the heater beams when the highest plasma temperatures can be expected. In contrast, the Cl line emission lasts considerably beyond the end of the backlighter pulse. The strongest emission observed by the spectrometer is for the Cl Ly-α line. This is also true when compared to the He-a line which was not covered by the spectral range of the streaked spectrometer. By varying the spot size of the backlighter beams we optimized both the conversion efficiency into Cl Ly-α, and minimized the strength of the red–shifted satellite with respect to the main Cl Ly-α line. At intensities of 1.8×10^{16} W/cm^2 we measured a contrast of 7.6. By increasing the intensity to 3.2×10^{16} W/cm^2 the contrast improved to 11.2 while the conversion efficiency stayed almost constant. For this experiment we chose a spot size of 150 μm emission yielding an intensity of XY $\times10^{16}$ W/cm^2. From the streak spectra it is evident that both the Cl Ly-α emission and the line contrast do not considerably change during the course of the backlighter beams. In contrast to that, the background noise on the main scattering spectrometer significantly changes during the backlighter pulse. It is decreasing toward the end of the backlighter pulse and thus the framing camera is gated late in probe pulse, as shown in Fig. 2. Due to the 100 μm mean free path at 3 keV, the x-ray photons scatter predominantly from a 40 μm-deep Be region on the undriven side. An 11° tilt is introduced so scattered 3 keV x-rays can exit towards the spectrometer with minimal reabsorption. The scattered signal is collected by a high throughput Bragg spectrometer using a highly oriented pyrolytic graphite (HOPG) crystal [9] which is mounted under 40° in for-

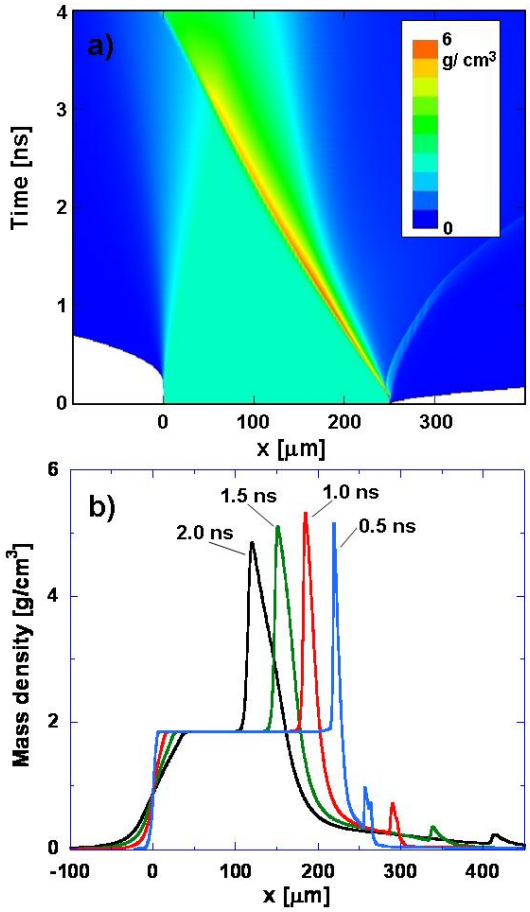

Figure 3: Mass density vs. time from 1D hydrodynamic simulations using Helios [10]. The heater beams are incident on the the silver foil from the right hand side and drive a shock into the beryllium. The shock velocity is determined to be 70 μm/ns.

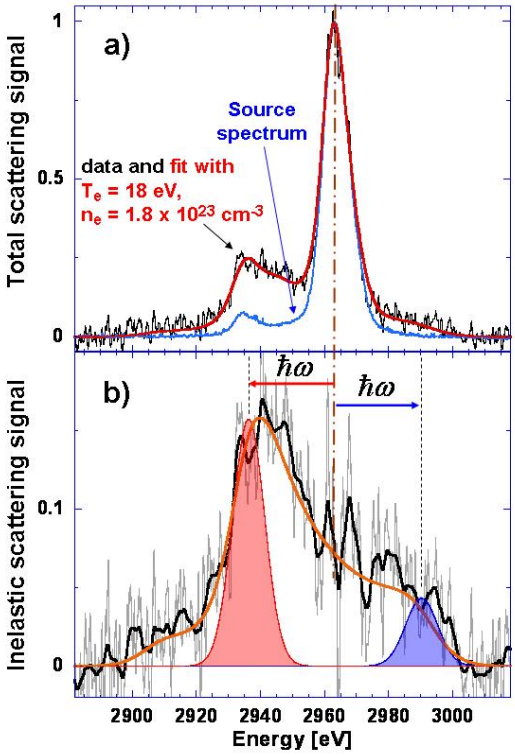

Figure 4: (a) Measured x-ray source and total scattering spectrum are shown along with the best fit (red line). (b) The lower panel shows inelastic scattered signal obtained by subtracting the source spectrum from the scattering spectrum. The fit was performed with the same plasma parameters as in panel (a). From the ratio of the up–shifted to the down–shifted plasmon signal the plasma temperature can be determined via the detailed balance relation. For details see text.

ward direction. For detection an x–ray framing camera is used with a 180 ps gate. The measured signal is read out by CCD camera fiber coupled to the framing camera. We flatfielded the spectrometer using bremsstrahlung emission from an aluminum plasma in order to account for reflectivity inhomogeneities of the HOPG crystal. Gold shields are used to block direct line and continuum emission from the plasmas generated by the heater and the backlighter beams. To assess the density uniformity in the plasma region probed by the x–ray source, we have performed 1D hydro simulations using HELIOS [10]. Fig. 3 shows the transient mass density. The heater beams are incident from the right hand side and start at t = 1 ns. A shock wave is launched and propagates with a velocity of 70 μm/ns through the Be foil. Hence at t = 1.6 ns, i.e. when the scattering signal is recorded, the shock has penetrated about 120 μm into the Be foil, and thus has not yet reached the plasma region which is probed by the x–ray backlighter.

3. Results and Discussion

The obtained scattering spectrum along with the source spectrum is shown in Fig. 4(a). The spectra are normalized to the Rayleigh peak at 2.962 keV. In addition to the down–shifted plasmon signal a clear inelastically scattered, up–shifted signal is observed. Fig. 4b shows the inelastically scattered signal which is obtained by subtracting the source spectrum from the scattered spectrum (Fig. 4a). The strength of the source is

adjusted such that the resulting inelastically scattered signal shows a smooth transition between the down-shifted and the up-shifted features as expected from simulations. In order to investigate the plasma temperature using the detailed balance relation (Eq. 1), two gaussian functions were fitted to the data. As constraints (1) their width is equal to that of the measured main Cl Ly-α line, and (2) their absolute energy shift with respect to the source line is equal, namely $\hbar|\omega_{res}| = 27.3$ eV, as indicated in Fig. 4b. The fit function on the down-shifted side is clearly more reliable due to the higher signal level. In particular, a very good agreement between the data and the fit is obtained for the rising edge at 2932 eV. On the blue-shifted side the experimental data seem to extend further out compared to the fit function. However, the deviation is on the order of magnitude which could be caused by the spectral spectrometer response function. Using Eq. 1 from the ratio of the two gaussians a plasma temperature of 21.1 eV is obtained. Considering an uncertainty of 15% for the blue shifted signal as the main source of error yields an uncertainty in T_e of $\Delta T_e = 3.7$ eV. The plasma density n_e can be inferred from the plasmon dispersion relation. For a classical collisionless plasma the dispersion was given by Bohm and Gross [11], which is valid for the long wavelength limit $\hbar k^2/(2m_e\omega) \ll 1$

$$\omega_{res}^2 \approx \omega_p^2 + \frac{3k_B T_e}{m_e} k^2, \qquad (2)$$

where ω_{res} is the resonance frequency obtained by the fitting procedure explained above, ω_p is the plasma frequency, and $k = 1.03$ Å^{-1} the momentum transfer. Using the electron temperature obtained from detailed balance, Eq. 2 yields a plasma density of $n_e = 1.7 \times 10^{23}$ cm^{-3}.

In the next step synthetic scattering spectra were generated and fitted to the experimental data. To model the spectra we used the RPA for the electron structure factor [12]. The source spectrum recorded on the Saran disk shot was used as the instrument function. The best agreement between the measured inelastic scattering signal (black curve) and the fit function (orange curve) could be obtained for $n_e = 1.8{\times}10^{23}$ cm^{-3} and an electron temperature of 18 eV, see Fig. 4b. In addition to that, from the ratio of the plasmon signal to the Rayleigh signal the ionization state and thus the mass density of the plasma can be determined. The strength of the Rayleigh peak depends on the ion structure factor which is calculated using the screened one component plasma model(SOCP, [Gregori2008]). Even though this has proven to yield the correct values for other systems (add examples), here we were not able to consistently

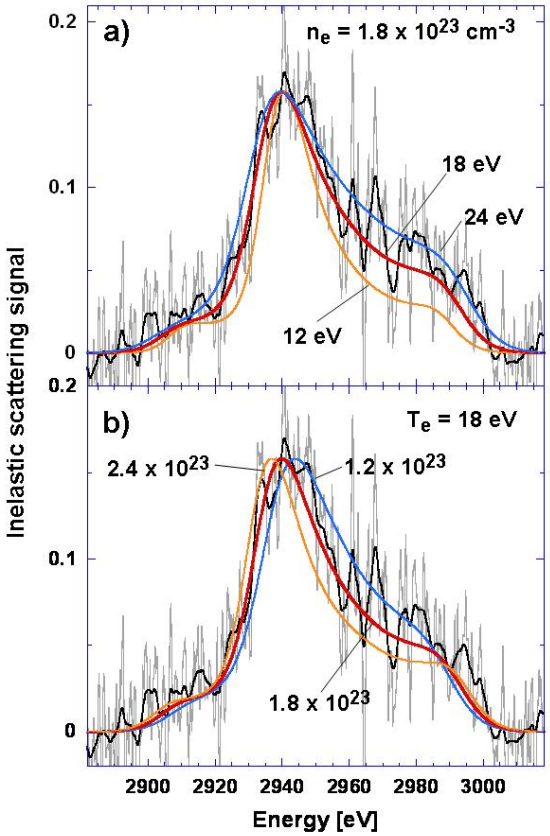

Figure 5: Sensitivity analysis for the electron temperature (a) and electron density (b).

model the spectra, in particular to obey the constraint $T_e = T_i$. If this constrained is lifted, a very good fit to the total scattering signal can be obtained, see Fig. 4a. For further analysis we assumed the ionization state to be $Z_f = 2.3$ as reported for similar plasma conditions [4]. At given electron density this corresponds to a mass density of 1.17 g cm^{-3} which is about 2/3 of solid Be. This suggests, that expansion of the Be has started before the x-ray probe arrives.

To illustrate the sensitivity of the inelastic scattering signal on the plasma parameters, Fig. 5 shows variations for T_e and n_e. The upper panel shows the variation with respect to temperature, and proves that in the plasma regime under study here the inelastically scattered signal is very sensitive to the electron temperature. This justifies the application of detailed balance for temperature measurement. The agreement with previously demonstrated methods is good and limited only by data

quality. Since detailed balance is based on first principle it will be very useful for testing models in the future.

Fig. 5b shows the dependence of the scattering signal on the electron density. Clearly, it is not as sensitive as on the plasma temperature. Significant variations occur only around the Rayleigh peak. To improve this future experiments will aim at higher plasma densities. This will be accomplished by timing the probe beam closer to the heater beams, and possibly by stronger heating to increase the ionization state.

4. Conclusion

A 250 μm Be was isochorically heated using Ag L–shell radiation. In the collective scattering regime an up– and a down–shifted plasmon signal were simultaneously measured for the first time. From detailed balance an electron temperature of 18 eV with an error of 25% could be inferred. Assuming a mean charge state of $Z = 2.3$, the mass density was deduced to be 1.20 ± 0.25 gcm^{-3}, significantly smaller than Be ground density. Future experiments will optimize the heating using thinner foils. Also, the plasma will be probed at an earlier time before significant expansion can occur.

Acknowledgments

This work was performed under the auspices of the U.S. Department of Energy by the Lawrence Livermore National Laboratory, through the Institute for Laser Science and Applications, under contract DE-AC52-07NA27344. The authors also acknowledge support from Laboratory Directed Research and Development Grants No. 08-LW-004 and 08-ERI-002.

References

[1] J. D. Lindl, P. Amendt, R. L. Berger, S. G. Glendinning, S. H. Glenzer, S. W. Haan, R. L. Kauffman, O. L. Landen, and L. J. Suter. The physics basis for ignition using indirect-drive targets on the national ignition facility. *Phys. Plasmas*, 11(2):339, 2004.

[2] A.L. Kritcher, P. Neumayer, J. Castor, T. Döppner, R.W. Falcone, O.L. Landen, H.J. Lee, R.W. Lee, E. Morse, A. Ng, S. Pollaine, D. Price, and S.H. Glenzer. Ultrafast x-ray thomson scattering of shock-compressed matter. *Science*, 322:69, 2008.

[3] S. H. Glenzer, G. Gregori, R. W. Lee, F. J. Rogers, S. W. Pollaine, and O. L. Landen. Demonstration of spectrally resolved x-ray scattering in dense plasmas. *Phys. Rev. Lett.*, 90(17):175002, 2003.

[4] S. H. Glenzer, O. L. Landen, P. Neumayer, R. W. Lee, K. Widmann, S. W. Pollaine, R. J. Wallace, G. Gregori, A. Höll, T. Bornath, R. Thiele, V. Schwarz, W. D. Kraeft, and R. Redmer. Observations of plasmons in warm dense matter. *Phys. Rev. Lett.*, 98(6):065002, 2007.

[5] H.J. Lee, P. Neumayer, J. Castor, T. Döppner, R.W. Falcone, C. Fortmann, B.A. Hammel, A.L. Kritcher, O.L. Landen, R.W. Lee, D.D. Meyerhofer, D.H. Munro, R. Redmer, S.P. Regan, S. Weber, and S.H. Glenzer. X-ray Thomson scattering measurements of density and temperature in shock-compressed beryllium. *Phys. Rev. Lett., in print*, 2009.

[6] S.H. Glenzer and R. Redmer. X-ray Thomson Scattering. *Rev. Mod. Phys., in print*, 2009.

[7] A. Höll, T. Bornath, L. Cao, T. Döppner, S. Düsterer, E. Förster, C. Fortmann, S. H. Glenzer, G. Gregori, T. Laarmann, K.-H. Meiwes-Broer, A. Przystawik, P. Radcliffe, R. Redmer, H. Reinholz, G. Röpke, R. Thiele, J. Tiggesbäumker, S. Toleikis, N. X. Truong, T. Tschentscher, I. Uschmann, and U. Zastrau. Thomson scattering from near-solid density plasmas using soft x-ray free electron lasers. *High Energy Density Physics*, 3(3):120, 2007.

[8] D. Pines and P. Nozieres. *The Theory of Quantum Fluids*. Addison-Wesley, Redwood City, CA, 1990.

[9] A. Pak, G. Gregori, J. Knight, K. Campbell, D. Price, B. Hammel, O. L. Landen, and S. H. Glenzer. X-ray line measurements with high efficiency bragg crystals. *Review of Scientific Instruments*, 75(10):3747, 2004.

[10] J. J. MacFarlane, I. E. Golovkin, and P. R. Woodruff. Helios-cr - a 1-d radiation-magnetohydrodynamics code with inline atomic kinetics modeling. *J QUANT SPECTROSC RA*, 99(1-3):381, 2006.

[11] D. Bohm and E. P. Gross. Theory of plasma oscillations.a. origin of medium-like behavior. *Physical Review*, 75(12):1851, 1949.

[12] G. Gregori, S. H. Glenzer, W. Rozmus, R. W. Lee, and O. L. Landen. Theoretical model of x-ray scattering as a dense matter probe. *Physical Review E*, 67(2), 2003.